CANCER DIAGNOSIS & PROGNOSIS *5*: 652-667 (2025)
doi: 10.21873/cdp.10482

Disulfidptosis-linked Gene Signatures Constitute Prognostic Models in Prostate Cancer

YASUO TAKASHIMA[1], KENGO YOSHII[2], MASAMI TANAKA[1] and KEI TASHIRO[1]

[1]Department of Genomic Medical Sciences, Kyoto Prefectural University of Medicine, Kyoto, Japan;
[2]Department of Mathematics and Statistics in Medical Sciences,
Kyoto Prefectural University of Medicine, Kyoto, Japan

Abstract

Background/Aim: Identification of cancer biomarkers for early detection is required. However, little is known about which candidate cell signaling pathway markers can be identified and which pathways may serve as therapeutic targets. We focused on the disulfidptosis among numerous signaling pathways, because it is a mechanism that causes cell death and is associated with iron-dependent cell death or ferroptosis, the tricarboxylic acid cycle, energy metabolism, and glucose uptake. The aim of the study was to detect the disulfidptosis-linked gene signatures associated with stage-specific makers and prognosis.

Materials and Methods: We examined the expression of 106 related genes in 324 patients with prostate cancer for disulfidptosis, a type of cell death triggered by disulfide stress resulting in disulfide bond-induced collapse of the cytoskeleton.

Results: The expression levels of *UBASH3B, ANP32E, PRC1, ACTB, SPG20,* and *DBN1* increased with cancer progression. Of these, *UBASH3B, PRC1,* and *ANP32E* were strongly expressed in cases with Gleason score ≥8. Conversely, the expression levels of *MYH13, FLNC, GLUD1, SAMM50, CHCHD3,* and *CAPZB* decreased. Of these, *GLUD1, CAPZB,* and *SAMM50* were decreased in cases with Gleason score ≥8. In addition, *UBASH3B, ANP32E, PRC1, DBN1, FLNC,* and *GLUD1* enabled the estimation of biochemical recurrence (BCR)-free survival. In particular, the prognostic formula comprising *ZHX2, SMPD4,* and *CHD4* using the Lasso-Cox regression model properly distinguished the BCR-free survival curves, indicating that these genes could be signatures for disulfidptosis.

Conclusion: Decoding disulfidptosis-related data in the transcriptome would provide crucial clues for finding novel approaches to personalized cancer medicine in prostate cancer.

Keywords: Prostate cancer, disulfidptosis, transcriptome, BCR-free survival, lasso-cox model.

Kei Tashiro, MD, Ph.D., Department of Genomic Medical Sciences, Kyoto Prefectural University of Medicine, 465 Kajii-cho, Hirokoji-agaru, Kawaramachi-dori, Kamigyo-ku, Kyoto 602-8566, Japan. Tel: +81 752515347, e-mail: tashiro@koto.kpu-m.ac.jp

Received August 7, 2025 | Revised September 10, 2025 | Accepted September 17, 2025

Introduction

Prostate cancer is the most diagnosed cancer in men worldwide and is the second leading cause of death in men (1, 2). Prostate-specific antigen (PSA) is a traditional marker for the diagnosis of prostate cancer but has low specificity (3). This is partly attributed to the difficulties in PSA detection in premalignant lesions, including prostatic intraepithelial neoplasia that has a lower concentration of serum PSA (3). Periostin is also a candidate biomarker for prostate cancer in the early stages and prostate cancer stroma in the advanced stages, owing to its increased expression during such contexts (4). Androgens and androgen receptor signaling have been shown to promote prostate cancer progression. Subsequently, androgen deprivation therapy has become the main therapy for patients with prostate cancer at different stages (5). However, a considerable proportion of patients receiving these treatments ultimately progresses to more aggressive disease, leading to the development of castration-resistant prostate cancer (5). Patients with prostate cancer frequently exhibit resistance to androgen deprivation therapy, a condition known as castration-resistant prostate cancer (5). Therefore, the identification of biomarkers for the early detection of prostate cancer is essential. However, little is known about which candidate cell signaling pathway markers can be identified and which pathways may serve as therapeutic targets.

Here, we focused on the disulfidptosis pathway among numerous signaling pathways. This is because disulfidptosis is a mechanism that causes cell death and is associated with iron-dependent cell death or ferroptosis, the tricarboxylic acid cycle, energy metabolism, and glucose uptake; in other words, it is called the Warburg effect (6, 7). Disulfidptosis is a novel type of cell death mediated by abnormal accumulation of intracellular disulfides and induced by glucose transporter inhibitors (8). It is triggered by the accumulation of reactive oxygen species (ROS) and relentless lipid peroxidation induced by disulfide-dependent mechanisms in tumor cells (9), and therefore, disulfidptosis suppresses tumor cell growth (10), suggesting a potential clinical application for use as advanced treatment strategy. Recent investigations have shed light on a distinctive form of programmed cell death known as disulfidptosis with high expression of *SLC7A11* (*SLC7A11*^{high}) (8). During glucose starvation, overabundant intracellular disulfides accumulate in *SLC7A11*^{high} cells, leading to an uncharacterized form that is distinct from apoptosis and ferroptosis (8). Simultaneously, F-actin collapses during glucose starvation, and aberrant disulfide bonds are induced in an *SLC7A11*-dependent manner (8). Additionally, glucose transporter inhibitors suppress *SLC7A11*^{high} tumor growth by downregulating disulfidptosis (8). Besides, *SLC7A11, SLC3A2, RPN1,* and *NCKAP1* have pivotal roles required for the progress of disulfidptosis in gastric cancer (11). A recent study showed that a disulfidptosis-related long non-coding RNA signature is a prognostic indicator for glioma immunotherapy (12) and that disulfidptosis-related genes could be potential prognostic biomarkers associated with tumor microenvironment and immunotherapy response (13). Long noncoding RNAs also contribute to establishing a prognostic risk prediction model in prostate cancer (14). However, promising biomarkers associated with disulfidptosis remain elusive in prostate cancer.

In this study, we analyzed transcriptomic and clinical data of prostate cancer patients to identify disulfidptosis-related signatures associated with prognosis. The genes were correlated with TNM stage, Gleason grade, and BCR-free survival. Here we would propose prognosis prediction models, and a hypothetical model in which disulfide stress may play roles in cell proliferation in prostate cancer. Findings from this study would suggest crucial roles in cell death or cell growth mechanisms induced by disulfide stress, offering insights into targeted therapies and personalized medicine.

Materials and Methods

Data collection. A dataset of gene expression and clinical information from patients with prostate cancer was used (15). Gene expression values of reads per kilobase of exon

per million mapped reads (RPKM) were subjected to subsequent analyses. Analyses were performed on 324 patients in the Prostate Cancer, German Cancer Research Center (Deutsches Krebsforschungszentrum, DKFZ) dataset (https://www.dkfz.de/en/frueherkennung-prostatakarzinom/index.php) (16), and representative results were validated using additional dataset of the Prostate Adenocarcinoma, The Cancer Genome Atlas (TCGA), PanCancer Atlas (494 patients) (https://data catalog.mskcc.org/dataset/10426) (16). Gene expression values of fragments per kilobase of exon per million mapped reads (FPKM) were subjected to subsequent analyses. Genes of interest (GOI) were annotated online using GOstat2.5 (http://gostat.wehi.edu.au/) (17) and Database for Annotation, Visualization, and Integrated Discovery (DAVID) 6.8 (https://david.ncifcrf.gov/) (18). Gene expression values were used directly for calculations and then graphed in appropriate applications (19, 20). However, the genes with RPKM=0 in all samples were excluded from all analyses. The workflow of this study is shown in Figure 1.

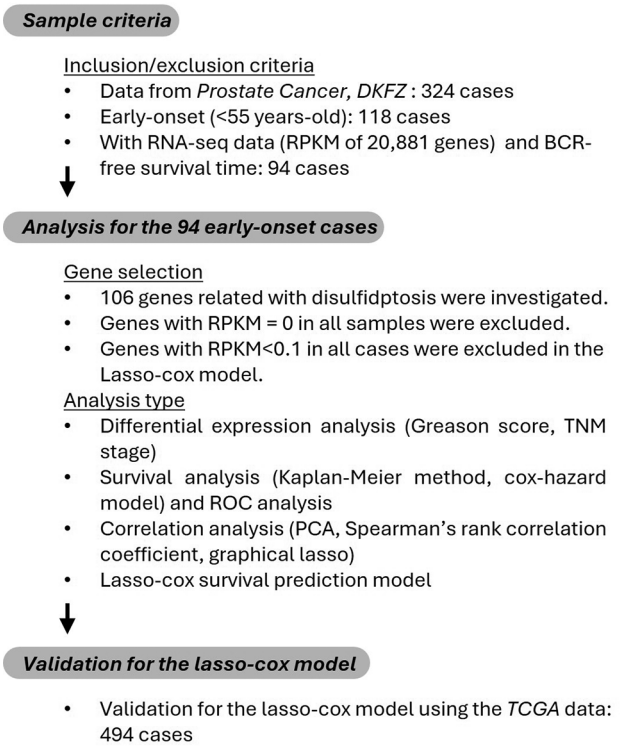

Figure 1. *Workflow of the study. Sample criteria and gene selection in the DKFZ, gene expression data used in this study, analysis type, and validation using the TCGA.*

Survival analysis. Correlations between gene expression and survival times were evaluated by Cox hazard regression analysis using R (16, 19, 21). Kaplan–Meier analysis was performed to estimate the survival distribution of the subgroups using R. Subgroups were divided by the median expression of GOI or median risk scores. The prognostic model genes were confirmed, and the risk scores were imputed as follows:

$$\text{Risk score}=\sum_{i=1}^{n} k_{i,coef} \times m_{i,RPKM}$$

where $k_{i,coef}$ indicates the Cox regression coefficient, i indicates prognostic gene candidates, and $m_{i,RPKM}$ indicates the gene expression level as RPKM (16). HR and CI were calculated using a Cox regression model according to patient survival times, which were assessed to compare the subgroups (22). BCR-free survival was defined as the time from the date of surgery for prostate cancer to the date of recurrence or the last follow-up.

Graphical lasso network analysis. Genetic interactions with hub networks among variables from gene expression were analyzed by graphical lasso estimation of Gaussian graphical models, such as a sparse inverse covariance matrix using a lasso (L1) penalty and the glasso package in R (16, 23).

Survey for therapeutic targets and drug responses. Drug responses in pan-cancer were surveyed with Gene Set Cancer Analysis (GSCA) online at https://guolab.wchscu.cn/GSCA/#/drug, based on the Genomics of Drug Sensitivity in Cancer (GDSC) dataset 1 and 2 (https://www.cancerrxgene.org/) and the Cancer Therapeutics Response Portal (CTRP) v2 dataset (https://portals.broadinstitute.org/ctrp/). Positive and negative correlations with false discovery rate (FDR) <0.05 indicated drug resistances and sensitivities in the subgroups harboring higher expression of GOI, respectively.

Statistics. Statistical analyses were performed using R4.3.3. *p*-Values <0.05 were considered statistically significant.

Results

Overview of analysis for disulfidptosis in prostate cancer. In this study, we developed a transcriptome-based prognosis prediction model for disulfidptosis, a type of cell death triggered by disulfide stress resulting in a disulfide bond-induced collapse of the cytoskeleton in prostate cancer, using the transcriptome data and clinical information of 324 patients (8, 16). In particular, the detailed expression profile of 106 disulfidptosis-related genes (24) (Figure 2) was investigated for the classification using TNM stage, Gleason score, BCR-free survival, and PSA levels. The 106 genes examined were mainly involved in actin filament binding (GO: 0051015, $p=4.69\times10^{-28}$), muscle filament sliding (GO: 0030049, $p=1.53\times10^{-15}$), cytoskeletal motor activity (GO: 0003774, $p=3.69\times10^{-17}$), and mitochondrial respiratory chain complex I assembly (GO: 0032981, $p=2.22\times10^{-11}$) and were associated with other functions and pathways including tight junction (KEGG: hsa04530, $p=6.70\times10^{-6}$), oxidative phosphorylation (KEGG: hsa00190, $p=9.85\times10^{-6}$), ferroptosis (KEGG: hsa04216, $p=1.65\times10^{-5}$), and chemical carcinogenesis - reactive oxygen species (KEGG:hsa05208, $p=6.11\times10^{-5}$).

AAAS	*EBLN2*	*LGALS13*	*PRC1*	*NDUFA10*	*TLN1*
ACTB	*EPAS1*	*LRPPRC*	*PRDX1*	*NDUFA11*	*TLN2*
ACTN1	*FANCI*	*ME1*	*RNH1*	*NDUFB10*	*TNKS1BP1*
ACTN2	*FLNA*	*MRPS17*	*RPA1*	*NDUFB11*	*TRIP6*
ACTN3	*FLNB*	*MYH1*	*RPN1*	*NDUFB6*	*UBASH3B*
ACTN4	*FLNC*	*MYH10*	*RRP1*	*NDUFC1*	*ZHX2*
ANP32E	*GCN1L1*	*MYH11*	*RUFY1*	*NDUFS1*	
ARMC6	*GLUD1*	*MYH13*	*SAFB*	*NDUFS2*	
ARNT	*GTF2I*	*MYH14*	*SAFB2*	*NIPBL*	
ATG5	*GYS1*	*MYH2*	*SAMM50*	*NLN*	
ATXN10	*HNRNPA3*	*MYH3*	*SART3*	*NSUN2*	
BOP1	*HNRNPH1*	*MYH4*	*SCO2*	*NUBPL*	
CAPZB	*HNRNPH2*	*MYH6*	*SLC3A2*	*OXSM*	
CD2AP	*HNRNPH3*	*MYH7*	*SLC7A11*	*PCBP1*	
CHCHD3	*HNRNPM*	*MYH7B*	*SMPD4*	*PCBP2*	
CHD4	*HNRNPU*	*MYH8*	*SPG20*	*PCBP3*	
CNOT1	*INF2*	*MYH9*	*SQSTM1*	*PDLIM1*	
DBN1	*IPO4*	*MYL6*	*STRAP*	*PML*	
DHX9	*IPO7*	*MYL6B*	*TARDBP*	*PPIH*	
DSTN	*IQGAP1*	*NCKAP1*	*TDP43*	*PPM1F*	

Figure 2. *A panel of the disulfidptosis-related genes examined in this study.*

Differential expression of the disulfidptosis-related genes during progression and metastasis. First, the 106 disulfidptosis-related genes were investigated during the progression and metastatic stages and compared with those of relatively early stage pT2a or Gleason grade 3+3 cases. Of these, *PRC1* expression was increased in pT3b (2.27-fold, $p=0.008$) cases and cases with Gleason grade 4+3 (2.11-fold, $p<0.001$) and ≥8 (2.85-fold, $p<0.001$) (Figure 3A). *FANCI* expression was also increased in cases with Gleason grade 4+3 (1.52-fold, $p=0.001$) and ≥8 (1.76-fold, $p=0.027$) (Figure 3A). However, the five genes were decreased in progression and metastatic stages as follows: *NSUN2* in pT2c (0.89-fold, $p=0.035$), *SPG20* in Gleason grade 4+3 (0.68-fold, $p=0.040$), *GLUD1* in pT3b (0.46-fold, $p=0.007$), pT4 (0.42-fold, $p=0.001$), and Gleason grade ≥8 (0.47-fold, $p=0.001$), *MYH11* in Gleason grade 4+3 (0.28-fold, $p=0.030$), and *DSTN* in pT3b (0.71-fold, $p=0.046$) and Gleason grade 4+3 (0.81-fold, $p=0.007$) cases (Figure 3B). These seven genes were considered progression marker candidates associated with disulfidptosis in prostate cancer progression. In addition, these genes were associated with the cytoplasm (GO: 0005737, $p=0.002$), cell cycle (UniProt: 0131, $p=0.004$), spindle (GO: 0005819, $p=0.036$), and actin filament binding (GO: 0051015, $p=0.055$) and were enriched in cytoskeletal regulators.

Similarly, metastatic stage-specific differential expression of these genes was examined. Genes with increased expression levels were as follows: *ANP32E* in pT4 (3.11-fold, $p=0.040$), *PCBP3* in pT4 (4.34-fold, $p=0.001$), *UBASH3B* in pT4 (2.23-fold, $p=0.031$) and Gleason grade ≥8 (1.65-fold, $p=0.031$), *ACTB* in pT4 (1.57-fold, $p=0.005$), and *DBN1* in Gleason grade ≥8 (1.62-fold, $p=0.041$) cases (Figure 4A). Conversely, genes with decreased expression were *NDUFS2* in Gleason grade ≥8 (0.92-fold, $p=0.036$),

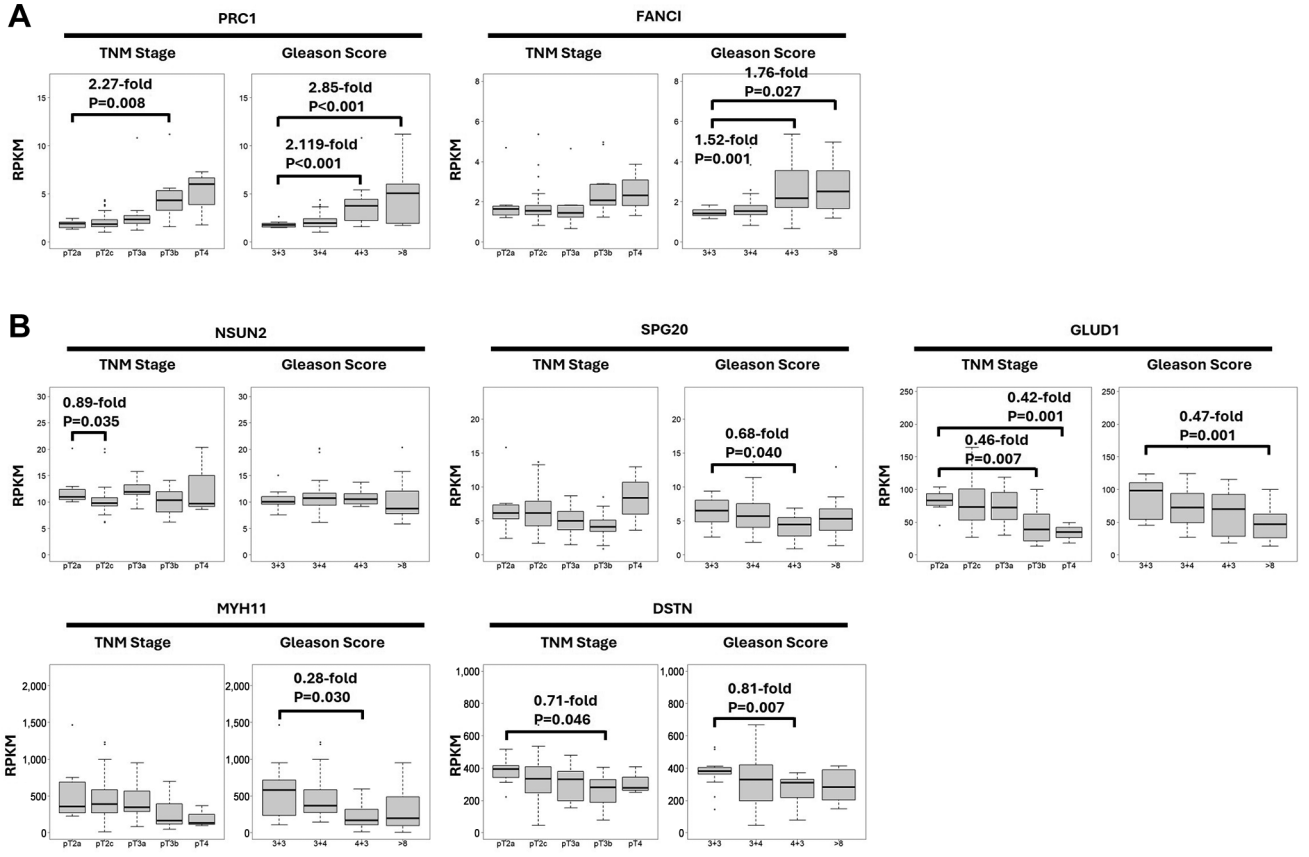

Figure 3. *Differential expression of disulfidptosis-related genes during progression of prostate cancer. (A) Increased expression levels of disulfidptosis-related genes PRC1 and FANCI in pT2c and pT3b cases compared with those in cases of pT2a and in cases with Gleason grade ≥4+3 compared with those in Gleason grade 3+3 cases. (B) Decreased expression levels of disulfidptosis-related genes NSUN2, SPG20, GLUD1, MYH11, and DSTN in pT2c and pT3b cases compared to those in pT2a cases and in Gleason grade ≥4+3 cases compared with those in Gleason score 3+3 cases. p-Values were computed using the Steel–Dwass multiple comparison test. RPKM: Reads per kilo base of transcript per million mapped reads.*

GYS1 in pT4 (0.55-fold, p=0.030), *TNSK1BP1* in Gleason grade ≥8 (0.62-fold, p=0.043), *C12orf51* in pT4 (0.38-fold, p=0.001), *FLNC* in pT4 (0.45-fold, p=0.040) and Gleason grade ≥8 (0.27-fold, p=0.032), *RPN1* in pT4 (0.73-fold, p=0.004) and Gleason grade ≥8 (0.80-fold, p=0.014), *TARDBP* in pT4 (0.91-fold, p=0.005), *MYH13* in pT4 (0.012-fold, p=0.008), and *CAPZB* in Gleason grade ≥8 (0.82-fold, p<0.001) cases (Figure 4B). These genes could be considered metastatic marker candidates associated with disulfidptosis in prostate cancer. These genes were also involved in cortical cytoskeleton (GO: 0030863, p<0.001), actin-binding (UniProt: 0009, p=0.002), cytoskeleton (GO: 0005856, p=0.002), methylation (UniProt: 0488, p=0.004), actin filament binding (GO: 0051015, p=0.005), and regulation of apoptotic process (GO: 0042981, p=0.006). This observation was interesting in apoptosis and methylation, compared to advanced stages.

Candidates of prognostic signatures with a single disulfidptosis-related gene. Next, the univariate Cox hazard regression analysis was used to clarify several candidates of prognostic signatures for BCR-free survival. These candidates included *ANP32E* [hazard ratio (HR)=0.28, 95% confidence interval (CI)=0.09-0.83, p=0.022], *ATG5* (HR=0.20, 95% CI=0.06-0.69, p=0.011), *DCTN* (HR=0.27, 95% CI=0.09-0.83, p=0.022), *IPO7* (HR=0.32, 95%

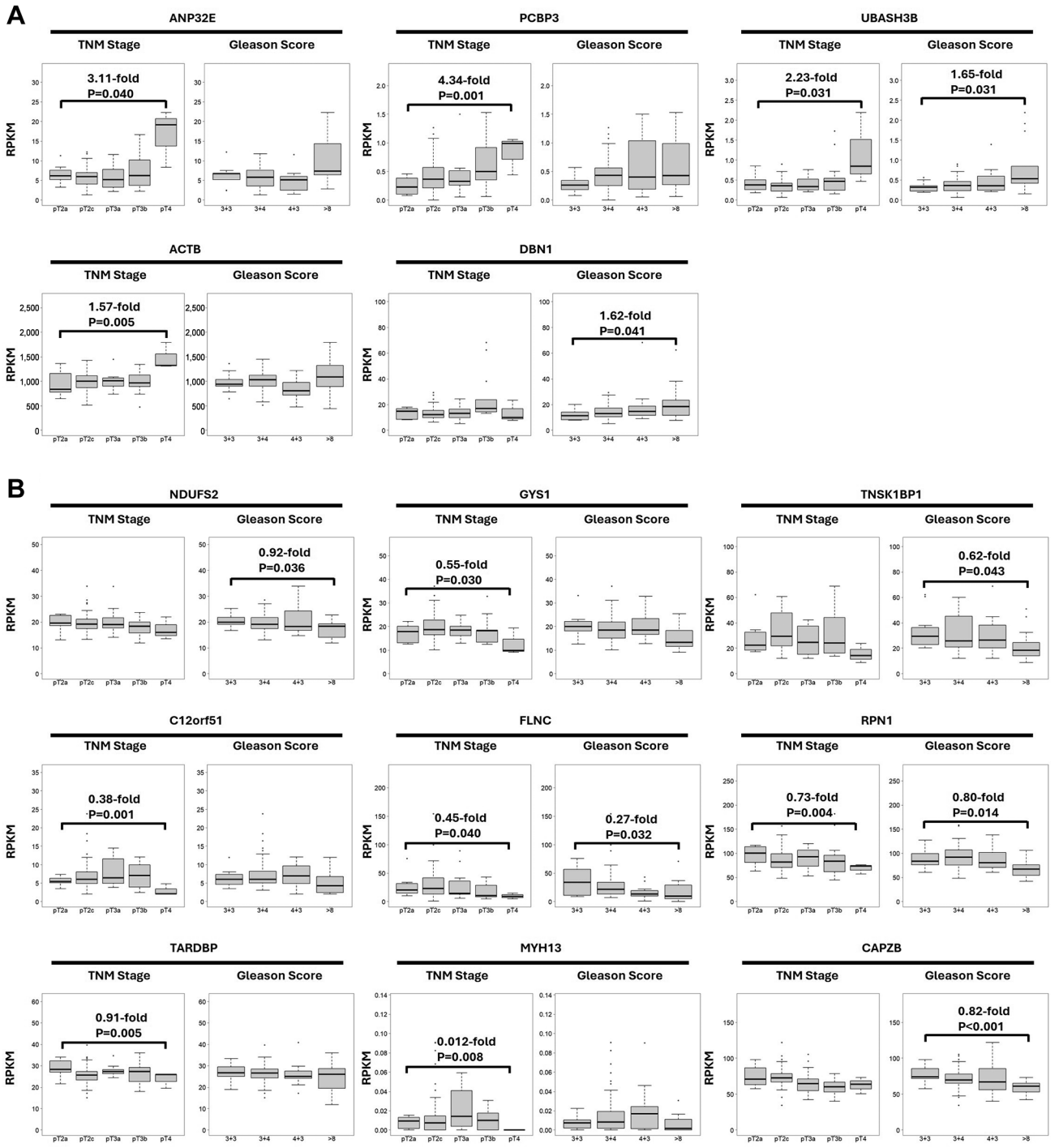

Figure 4. *Differential expression of disulfidptosis-related genes during metastasis of prostate cancer. (A) Increased expression levels of disulfidptosis-related genes ANP32E, PCBP3, UBASH3B, ACTB, and DBN1 in pT4 cases compared to those in pT2a cases and in cases with Gleason grade ≥8 compared to those in Gleason grade 3+3 cases. (B) Decreased expression levels of disulfidptosis-related genes NDUFS2, GYS1, TNSK1BP1, C12orf51, FLNC, RPN1, TARDBP, MYH13, and CAPZB in pT4 cases compared with those in pT2a cases and in Gleason grade ≥8 cases compared with those in Gleason grade 3+3 cases. p-Values were computed using the Steel–Dwass multiple comparison test. RPKM: Reads per kilo base of transcript per million mapped reads; ND: not detected.*

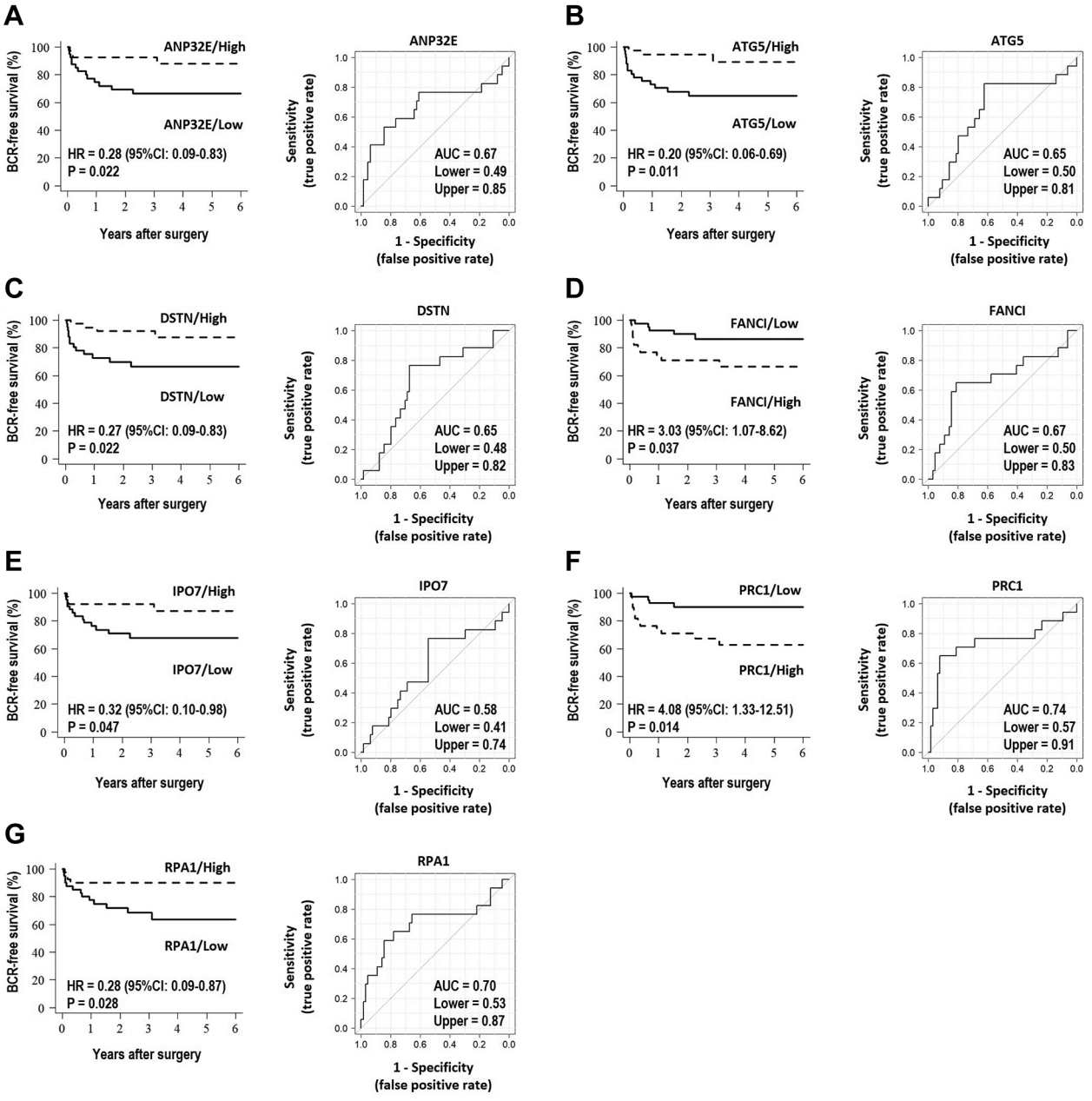

Figure 5. *Candidate disulfidptosis-related genes for prognosis prediction using univariate Cox hazard model in prostate cancer. (A) ANP32E; (B) ATG5; (C) DSTN; (D) FANCI; (E) IPO7; (F) PRC1; (G) RPA1. (left panel) BCR-free survival rates were estimated using univariate Cox hazard analysis. High and low indicate the subgroups with higher and lower expression levels, respectively, compared to the median expression level of the gene. HR: Hazard ratio; CI: confidential interval. (Right panel) Receiver operating characteristic (ROC) analysis for BCR-free survival times. The area under the curve (AUC) is calculated.*

CI=0.10-0.98, *p*=0.047), and *RPA1* (HR=0.28, 95% CI=0.09-0.87, *p*=0.028) as better prognosis factors (Figure 5A-C, E, and G), and *FANCI* (HR=3.03, 95% CI=1.07-8.62, *p*=0.037) and *PRC1* (HR=4.08, 95%CI=1.33-12.51, *p*=0.014) as poor prognosis factors (Figure 5D and F). Besides, the receiver operating characteristic (ROC) curve analysis showed the

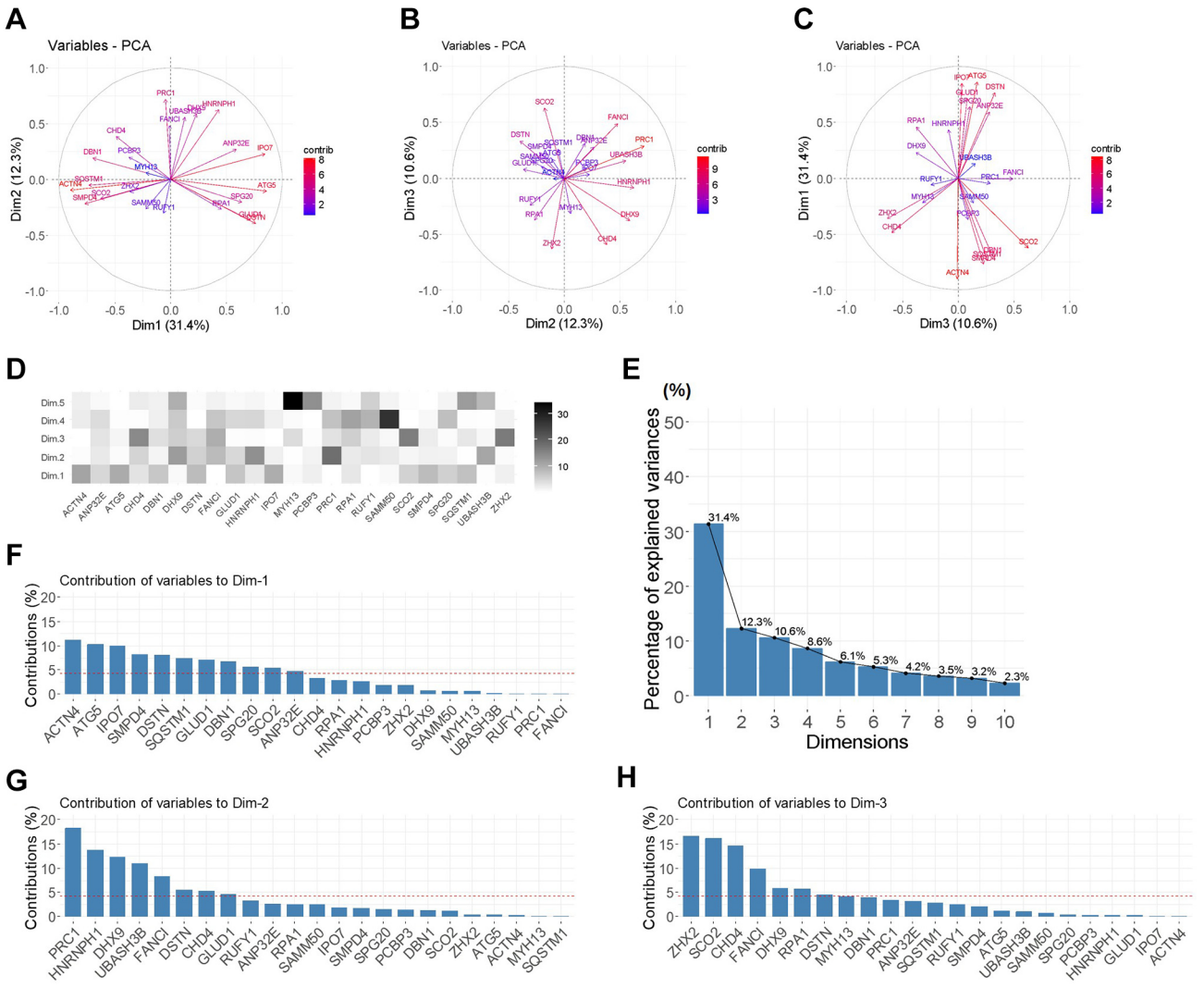

Figure 6. *PCA of the representative genes involved in disulfidptosis in prostate cancer. (A-C) Biplots of the principal components generated from the representative genes. (A) Dimension (Dim)1 and Dim2. (B) Dim2 and Dim3. (C) Dim3 and Dim1. Color configurations represent contributions as high (red) to low (blue). (D) A library of five representative principal components generated from the disulfidptosis-related genes. Color configurations represent contributions as high (black) to low (white). (E) Percentage contribution explains the variances of the dimensions. (F-H) The contributions of the representative variables of dimensions. Dim1 (F), Dim2 (G), and Dim3 (H). Red-dashed lines on the graph indicate expected average contributions. PCA: Principal component analysis.*

following areas under the curves (AUCs): *ANP32E* (AUC=0.67, 95% CI=0.49-0.85), *ATG5* (AUC=0.65, 95% CI=0.50-0.81), *DSTN* (AUC=0.65, 95% CI=0.48-0.82), *IPO7* (AUC=0.58, 95% CI=0.41-0.74), and *RPA1* (AUC=0.70, 95% CI=0.53-0.83) (Figure 5A-C, E, and G). For the poor prognosis factors, the results were as follows: *FANCI* (AUC=0.67, 95% CI=0.50-0.83) and *PRC1* (AUC=0.74, 95% CI=0.57-0.91) (Figure 5D and F). These gene expression patterns could be used as appropriate prognostic indicators of disulfidptosis in prostate cancer.

Principal component analysis for the expression of disulfidptosis-related genes. The disulfidptosis-related genes were also classified into several subgroups using

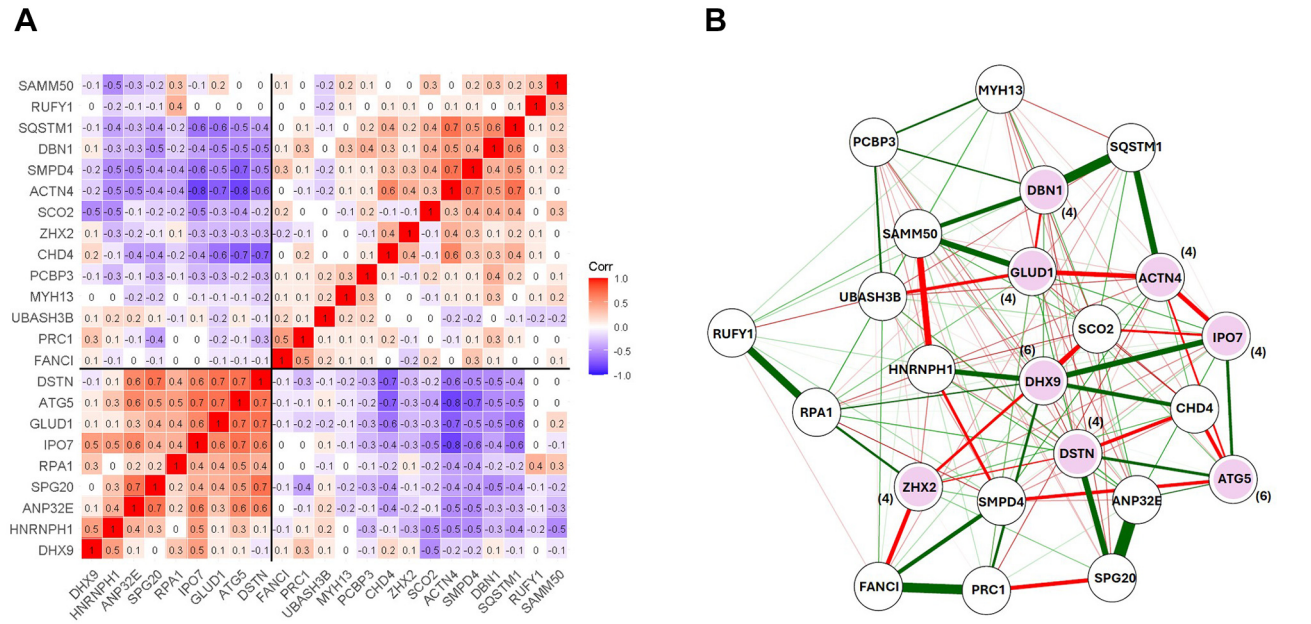

Figure 7. *Correlations between the expression levels of disulfidptosis-related genes in prostate cancer. (A) Coexpression patterns of the representative genes involved in disulfidptosis. Color configurations represent contributions with Spearman's rank correlation coefficient as direct (red) to inverse (blue). (B) A disulfidptosis-related gene network generated from the graphical lasso model based on the coexpression patterns of the genes. Thick and thin lines represent relatively strong and weak binding, respectively, with direct (green) or inverse correlation (red). The numbers in the parenthesis indicate the numbers of edges of the nodes. Highlighted circles represent candidates in the hub harboring >3 edges (weight >0.15).*

principal component analysis (PCA). The PCA biplots indicated that the top three dimensions (Dim) included Dim1, Dim2, and Dim3 (Figure 6A-C). Furthermore, by adding Dim4 and Dim5, the matrix of the five principal components was summarized (Figure 6D). The following dimension classification of the genes were obtained: Dim1 harbored *ACTN4* (relative percent contribution to the dimension: 11.23%), *ATG5* (10.29%), *IPO7* (9.99%), *SMPD4* (8.18%), *DSTN* (8.10%), *GLUD1* (7.07%), *DBN1* (6.73%), and *ANP32E* (4.84%), associated with acetylation (UniPlot: 0007, p=0.0012), actin cytoskeleton (GO: 0015629, p=0.003), actin-binding (UniPlot: 0009, p=0.006; GO:0003779, p=0.006), and cytoplasm (GO: 0005737, p=0.019); Dim2 harbored *PRC1* (18.21%), *HNRNPH1* (13.75%), *DHX9* (12.24%), and *UBASH3B* (10.94%), associated with identical protein binding (GO: 0042802, p=0.023) and nucleus (GO: 0005634, p=0.025; UniPlot:0539, p=0.034); and Dim3 harbored *ZHX2* (16.64%), SCO2 (16.22%), *CHD4* (14.60%), and *FANCI* (9.87%) associated with chromatin (GO: 0000785, p=0.008), DNA binding (GO: 0003677, p=0.014), isopeptide bond (UniPlot: 1017, p=0.047), and metal ion binding (GO: 0046872, p=0.057). In addition, Dim4 included *SAMM50* (27.22%), *RPA1* (11.43%), *RUFY1* (9.31%), and *SPG20* (7.80%), whereas Dim5 included *MYH13* (34.31%), *SQSTM1* (12.20%), and *PCBP3* (13.77%). The Dim5-relevant genes were associated with extracellular exosomes (GO: 0070062, p=0.011); however, Dim4-relevant genes were not detected in statistically significant ontology terms. Additionally, the analysis of the percentage contribution of the dimensions showed five representative dimensions with >5% contribution (Figure 6E). The percentage contributions of Dim1, Dim2, and Dim3 were highly consistent with the biplot results (Figure 6F-H). These results suggested that the examined disulfidptosis-related genes were successfully distinguished into five main subgroups using PCA.

Approximate combined classification using expression correlation and graphical lasso network. Twenty-three representative genes were extracted from the results of differential expression patterns, Kaplan–Meier survival curves, ROC curves, and percent contributions to principal components. The matrix of correlation patterns of the genes was divided into two subgroups (Figure 7A). This indicates that the 23 representative genes could be divided into two subgroups. The first group included *DHX9, HNRNPH1, ANP32E, SPG20, RPA1, IPO7, GLUD1, ATG5*, and *DSTN*. The second group included *FANCI, PRC1, UBASH3B, MYH13, PCBP3, CHD4, ZHX2, SCO2, ACTN4, SMPD4, DBN1, SQSTM1, RUFY*, and *SAMM50*. In contrast, the graphical lasso model constituted a dense hub network including *ATG5, DHX9, ACTN4, DBN1, DSTN, GLUD1, IPO7*, and *ZHX2* (edge number >4, edge weight >0.15) (Figure 7B). Interestingly, the positive correlation cluster that included *DHX9, IPO7, GLUD1, ATG5*, and *DSTN* was negatively associated with another positive correlation cluster that included *ZHX2, ACTN4*, and *DBN1*. These results suggested that there are approximately two cellular or molecular functions that reciprocally support disulfidptosis in prostate cancer.

A construction of the lasso-cox prognostic prediction model with disulfidptosis-related genes. These 23 genes were used to reduce the sparse groups in the lasso analysis (Figure 8A and B). Eleven genes with estimated HRs (Figure 7C) were used for the multivariate Cox regression analysis (Figure 8D). Finally, by using coefficient (Coef) values with $p<0.05$ in the cox analysis, prognosis prediction formula was obtained as: Risk score=−2.76 *ZHX2* + 1.50 *SMPD4* + 1.15 *CHD4*. The subgroup with scores higher than the median risk score exhibited shorter BCR-free survival times than the subgroup with lower scores (HR=5.43, 95% CI=1.56-18.93, $p=0.008$) (Figure 8E).

These results suggested that the three representative genes could be effective in predicting BCR-free survival, that is, progression of prostate cancer. The similar results were nearly replicated in disease-free survival (DFS) (HR=2.51, 95% Cl=0.89-7.08), $p=0.082$) of the patients with tumor stages T3 and T4 in the Prostate Adenocarcinoma, TCGA, PanCancer Atlas. On the other hand, statistically significant hazard ratios were validated in overall survival (OS) of all patients (HR=1.74, 95% CI=1.21-2.51, $p=0.003$) and the patients with tumor stages T3 and T4 (HR=1.43, 95% CI=1.01-2.03, $p=0.043$), disease-specific survival (DSS) of all patients (HR=1.82, 95% CI=1.18-2.79, $p=0.007$), and the patients with tumor stages T3 and T4 (HR=1.89, 95% CI=1.23-2.91, $p=0.004$), progression-free survival (PFS) of all patients (HR=1.63, 95% CI=1.13-2.34, $p=0.009$) and the patients with tumor stages T3 and T4 (HR=1.63, 95% CI=1.14-2.34, $p=0.008$) in the TCGA, PanCancer Atlas dataset. Thus, it is possible to predict several survival times with some subgroups in prostate cancer using a mixed expression model including *ZHX2, CHD4,* and *SMPD4*. However, statistically significant HRs were estimated even if *SMPD4* was excluded from formulas with the three gene candidates, so it may be possible for a better combination of genes to exist. Since these results show statistical prognostic prediction models on the gene expression levels, the importance as molecular markers and biological significance of genes should be clarified *in vitro* and *vivo* experiments in future. Alternatively, it would be explored in prospective cohort studies.

Discussion

A previous study emphasized several forms of programmed cell death, such as apoptosis, ferroptosis, pyroptosis, and cytoproptosis, which exhibit unique morphological, biochemical, and functional traits (25). Programmed cell death can be divided into suicide and sabotage programs (25). However, the boundaries between the two are vague, and these mechanisms may intersect or overlap under certain circumstances (26). The most recently discovered type of programmed cell death is disulfide stress-induced cell death, which is marked by an abnormal buildup of disulfide bonds in intracellular molecules and proteins (8). Apoptosis is typically repressed in tumor cells, which is one of the causes of their infinite cell proliferation; however, in

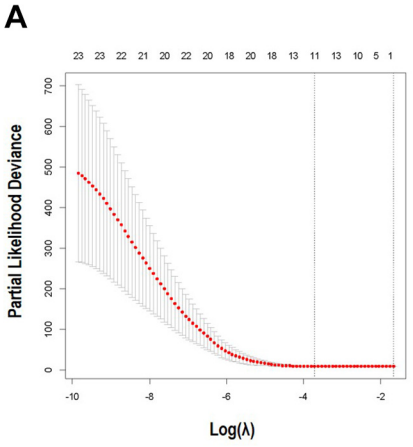

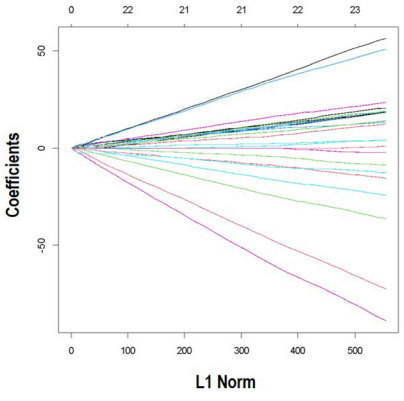

C

Symbol	Hazard ratio
SMPD4	1.95
CHD4	1.64
SQSTM1	1.50
HNRNPH1	1.28
DHX9	1.23
RPA1	0.86
SPG20	0.66
ZHX2	0.23

D

	Coef	Hazard ratio	Lower 95%CI	Upper 95%CI	*p* value
ZHX2	-2.76	0.06	0.02	0.24	<0.001
SMPD4	1.50	4.47	1.78	11.20	0.001
CHD4	1.15	3.15	1.31	7.55	0.010
HNRNPH1	0.51	1.67	0.87	3.19	0.125
SPG20	-0.77	0.46	0.16	1.34	0.156
RPA1	-0.56	0.57	0.21	1.55	0.274
DHX9	0.30	1.35	0.72	2.56	0.349
SQSTM1	0.34	1.40	0.69	2.87	0.355

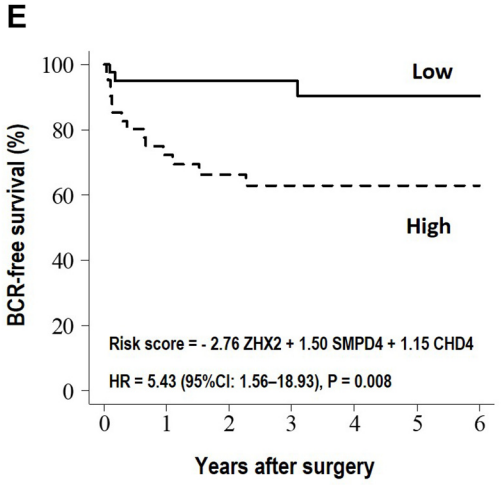

Figure 8. *Construction of the prognosis prediction model using the lasso-Cox model. (A) Partial likelihood deviance vs lambda relationship in the lasso model. (B) Coefficients against L1 norm lasso coordinate descent for sparse group. (C) Resultant factors with hazard ratios estimated by univariate Cox hazard regression analysis for BCR-free survivals. (D) Summary of the multivariate Cox hazard regression analysis performed using the data of eleven genes from the lasso. Coef: Coefficient; CI: confidence interval. (E) The prognosis prediction model (risk score) developed based on the lasso-Cox model for BCR-free survival in prostate cancer. HR: Hazard ratio; CI: confidence interval. High and low groups were divided by the median of risk score from the model.*

some cases, it causes various types of cell death, including disulfidptosis. In this study, we showed the first construction of a prognosis prediction model based on disulfidptosis in prostate cancer.

Here, we present a disulfidptosis-related prognostic signature for prostate cancer. From the expression profiles of cancer progression and metastasis stages, *PRC1* and *FANCI* levels increased with cancer grade and were associated with shorter BCR-free survival times. Increased PRC1 protein levels have been observed during the S and G_2/M phases of the cell cycle, followed by a dramatic decrease at the mitotic exit and entrance into the G1 phase (27, 28). The FANCI protein participates in the meiotic recombination of germ cells (29), and deletion of the *Fanci* gene causes a strong meiotic phenotype and severe hypogonadism (30). Therefore, these genes are likely reliable prognostic factors. MYH11 and MYH13 are hexameric proteins that consist of two heavy-chain subunits and two pairs of non-identical light-chain subunits (31-33). MYH family members are major

contractile proteins that convert chemical energy into mechanical energy via hydrolysis of ATP (26, 34). Cancer metastasis requires cytoskeletal flexibility, and relevant gene alterations are likely to influence patient survival. Considering their molecular functions and possible contributions to lifespan, decreased *MYH11* and *MYH13* expression levels in the prostate cancer transcriptome during advanced and metastatic stages may reciprocally contribute to cell migration and/or invasion through cell plasticity and energy metabolism for morphological change and cell movement, respectively. ANP32E is an ANP32 family member that shares N-terminal leucine-rich repeats and a C-terminal variable anionic region and forms a complex with SET domain proteins that stabilize short-lived mRNAs containing AU-rich elements (35). ANP32E also has an acetyltransferase inhibitory activity, which plays a role in chromatin remodeling and transcription (35). In the present study, *ANP32E* mRNA was increased in the metastatic stage, and the subgroup with higher expression of *ANP32E* showed better prognosis, which is consistent with its function as a transcriptional repressor. However, why *ANP32E* is increased in the metastatic stage, which seems contradictory, is hard to specify and will need further investigations *in vitro* and *vivo*. ZHX2 or CHD4 repress transcriptional activity by interacting with the A subunit of nuclear factor-Y (NF-YA) (36) or constituting the nucleosome remodeling and deacetylase (NuRD) complex for epigenetic alteration (37-39), respectively. Sphingomyelin phosphodiesterase 4 (SMPD4) induces epithelial-mesenchymal transition, which is also a late-stage marker of clear cell renal cell carcinoma (ccRCC) (40). Thus, a selection of extremely unique genes may construct a hypothetical model. Briefly, disulfide stress induces epithelial-mesenchymal transition (EMT) with SMPD4, and represses tumor suppressor genes [*e.g.*, *BRCA2, CDKN1A* (*$p21^{CIP1/WAF1}$*), *CDKN1B* (*$p27^{KIP1}$*), *FOXO1, LATS2, NKX3.1, PTEN, RB1, TP53, and ZBTB16* (*PLZF*) in prostate cancer] with the transcriptional repression complex ZHX2-NF-YA targeting the CCAAT DNA motif, and the chromatin remodeling complex CHD4-NuRD targeting the methylated CpG island, thereby guaranteeing tumor cell proliferation (Figure 9A and B). Therefore, the three genes are related to cancer proliferation with EMT and chromatin remodeling, which may be associated with disulfidptosis. Our findings provide insights into the biological significance of disulfidptosis in cancer resistance.

Furthermore, expression analyses for drug responses in pan-cancer return the results as sensitive to prostatic adenocarcinoma cells *in vitro* as follows: Histone deacetylase (HDAC) inhibitors including Vorinostat (FDR=1.04×10^{-20}), AR-42 (FDR=1.16×10^{-20}, CAY10603 (FDR=1.02×10^{-18}), and Belinostat (FDR=4.27×10^{-15}) in *$CHD4^{high}$*; Vorinostat (FDR=7.74×10^{-4}) in *$SMPD4^{high}$*; and CUDC-101 (FDR=8.40×10^{-8}) in *$ZHX2^{high}$*. Similarly, pan-cancer cell lines also indicate sensitivities for protein kinase inhibitors including NPK76-II-72-1 (FDR=1.81×10^{-18}) and BX-912 (FDR=5.79×10^{-13}) in *$CHD4^{high}$*; NPK76-II-72-1 (FDR=2.51×10^{-4}), TG101348 (FDR=1.03×10^{-3}), TPCA-1 (FDR=1.76×10^{-3}), BX-912 (FDR=1.88×10^{-3}), GSK1070916 (FDR=2.50×10^{-3}), and KIN001-260 (FDR=4.76×10^{-3}) in *$SMPD4^{high}$*; ZSTK474 (FDR=2.63×10^{-9}), GSK690693 (FDR=3.82×10^{-9}), AZD6482 (FDR=7.87×10^{-9}), EKB-569 (FDR=1.44×10^{-8}), THZ-2-49 (FDR=1.49×10^{-7}), GSK2126458 (FDR=2.49×10^{-7}), PHA-793887 (FDR=5.52×10^{-7}),and PIK-93 (FDR=1.02×10^{-6}) in *$ZHX2^{high}$*. However, various mitogen-activated protein kinase (MAPK) kinase (MEK) inhibitors show resistance in *$CHD4^{high}$*, *$SMPD4^{high}$*, and *$ZHX2^{high}$*. These suggest a possibility that HDAC inhibitors may be effective to prostate cancer, but MEK inhibitors may not so, which is a hint for selective drugs in prostate cancer treatment and compatibilities/affinities with disulfidptosis-related signaling and chromatin remodeling but not MAPK-dependent cancer cell proliferation.

Recent studies have highlighted key molecular factors that may improve the diagnosis, prognosis, and treatment of prostate cancer. Huang *et al.* identify a significant association between the DNMT3A rs77993651 variant and survival outcomes in patients undergoing androgen deprivation therapy (ADT), suggesting DNMT3A as a potential prognostic biomarker and therapeutic target (41). Nakamura *et al.* explore early diagnostic biomarkers and find that *BMP7* expression is significantly reduced in

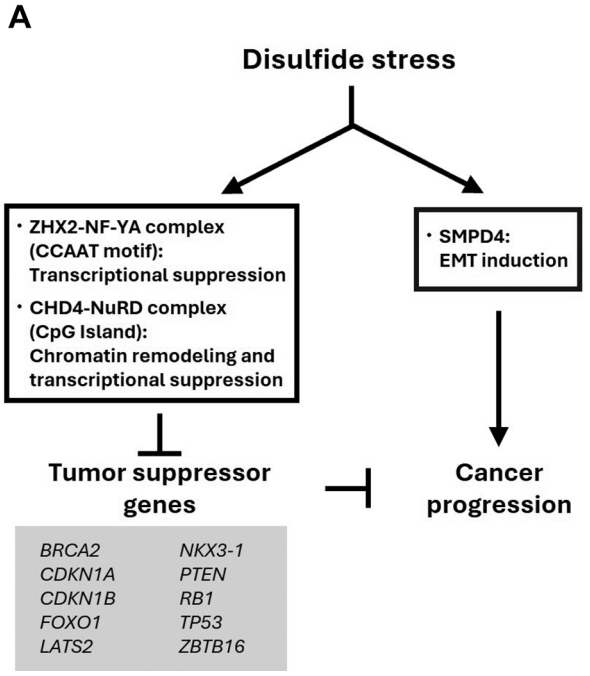

B

	CCAAT motif within 10 kb from TSS		CpG island within 100 kb from TSS
	CCAAT/ATTGG	Total	CpG Island
BRCA2	8/5	13	chr13: 32311288-32311525
CDKN1A	9/11	20	chr6: 36594131-36594635
			chr6: 36660810-36661220
CDKN1B	9/2	11	chr12: 12561700-12562924
FOXO1	10/7	17	chr13: 40664364-40667613
LATS2	4/9	13	chr13: 21060381-21061768
NKX3-1	6/6	12	chr8: 23682295-23683089
PTEN	6/7	13	chr10: 87862016-87862839
RB1	7/14	21	chr13: 48303324-48304365
TP53	7/8	14	chr17: 7688177-7688521
ZBTB16	5/8	13	chr11: 114058912-114061468

TSS: transcriptional start site, chr: chromosome

Figure 9. *A hypothetical model of cancer progression strategy constituted by the three candidates of disulfidptosis-related prognostic factors. (A) Disulfide stress induces epithelial-mesenchymal transition (EMT) and represses tumor suppressor genes by a transcriptional repression complex and chromatin remodeling, thereby guaranteeing tumor cell proliferation. (B) The CCAAT/ATTGG DNA motif and CpG island nearby transcriptional start site of 10 representative tumor suppressor genes in prostate cancer.*

prostate cancer tissues, indicating the potential utility in early detection (42). Meanwhile, *RHAMM* expression enhances prostate cancer cell migration and is associated with poor prognosis, proposing *RHAMM* as a novel prognostic marker in metastatic hormone-sensitive prostate cancer (43). In this way, recent findings show promising indications for improving clinical management through molecular profiling in prostate cancer. This study would add prognostic factors linked to disulfidptosis in prostate cancer.

Conclusion

Based on the promising results from previous and current studies, disulfidptosis may have great prospects in the treatment of tumors, including prostate adenocarcinomas. However, due to limited studies, the underlying mechanism of disulfidptosis and the relevant phenomena remain largely unknown. Additionally, the clinical significance and value of disulfidptosis-related genes remain uncertain. Therefore, it is necessary to assess the roles of disulfidptosis-linked genes in tumor cells. Because disulfidptosis represents a novel form of programmed cell death, the detailed mechanisms by which disulfide stress triggers cell death in tumors remain unclear. Therefore, future molecular and animal studies are required. The novel hypothetical model for prostate cancer cell proliferation proposed in this study should also be verified through *in vitro* and animal experiments. The clinical relevance of disulfidptosis in human prostate cancer also requires further investigation.

Data Availability

The datasets used in the study are available from the Prostate Cancer at DKFZ and the Prostate Adenocarcinoma at TCGA.

Conflicts of Interest

The Authors declare no conflicts of interest.

Authors' Contributions

Y.T. designed the experiments. Y.T., K.Y. and M.T. performed the experiments. Y.T., K.Y. and M.T. analyzed data. Y.T., K.Y., M.T. and K.T. wrote the manuscript.

Funding

This study was supported in part by MEXT/JSPS KAKENHI (23K08528) to Y.T. The funder had no role in the study design, data collection and analysis, decision to publish, or preparation of the manuscript.

Artificial Intelligence (AI) Disclosure

No artificial intelligence (AI) tools, including large language models or machine learning software, were used in the preparation, analysis, or presentation of this manuscript.

References

1 Torre LA, Bray F, Siegel RL, Ferlay J, Lortet-Tieulent J, Jemal A: Global cancer statistics, 2012. CA Cancer J Clin 65(2): 87-108, 2015. DOI: 10.3322/caac.21262

2 Calcinotto A, Spataro C, Zagato E, Di Mitri D, Gil V, Crespo M, De Bernardis G, Losa M, Mirenda M, Pasquini E, Rinaldi A, Sumanasuriya S, Lambros MB, Neeb A, Lucianò R, Bravi CA, Nava-Rodrigues D, Dolling D, Prayer-Galetti T, Ferreira A, Briganti A, Esposito A, Barry S, Yuan W, Sharp A, de Bono J, Alimonti A: IL-23 secreted by myeloid cells drives castration-resistant prostate cancer. Nature 559(7714): 363-369, 2018. DOI: 10.1038/s41586-018-0266-0

3 Alexander EE, Qian J, Wollan PC, Myers RP, Bostwick DG: Prostatic intraepithelial neoplasia does not appear to raise serum prostate-specific antigen concentration. Urology 47(5): 693-698, 1996. DOI: 10.1016/s0090-4295(96)00004-0

4 Doldi V, Lecchi M, Ljevar S, Colecchia M, Campi E, Centonze G, Marenghi C, Rancati T, Miceli R, Verderio P, Valdagni R, Gandellini P, Zaffaroni N: Potential of the stromal matricellular protein periostin as a biomarker to improve risk assessment in prostate cancer. Int J Mol Sci 23(14): 7987, 2022. DOI: 10.3390/ijms23147987

5 Watson PA, Arora VK, Sawyers CL: Emerging mechanisms of resistance to androgen receptor inhibitors in prostate cancer. Nat Rev Cancer 15(12): 701-711, 2015. DOI: 10.1038/nrc4016

6 Takashima Y, Hayano A, Yamanaka R: Metabolome analysis reveals excessive glycolysis via PI3K/AKT/mTOR and RAS/MAPK signaling in methotrexate-resistant primary CNS lymphoma-derived cells. Clin Cancer Res 26(11): 2754-2766, 2020. DOI: 10.1158/1078-0432.CCR-18-3851

7 Wang LY, Liu XJ, Li QQ, Zhu Y, Ren HL, Song JN, Zeng J, Mei J, Tian HX, Rong DC, Zhang SH: The romantic history of signaling pathway discovery in cell death: an updated review. Mol Cell Biochem 479(9): 2255-2272, 2024. DOI: 10.1007/s11010-023-04873-2

8 Liu X, Nie L, Zhang Y, Yan Y, Wang C, Colic M, Olszewski K, Horbath A, Chen X, Lei G, Mao C, Wu S, Zhuang L, Poyurovsky MV, James You M, Hart T, Billadeau DD, Chen J, Gan B: Actin cytoskeleton vulnerability to disulfide stress mediates disulfidptosis. Nat Cell Biol 25(3): 404-414, 2023. DOI: 10.1038/s41556-023-01091-2

9 Zheng P, Zhou C, Ding Y, Duan S: Disulfidptosis: a new target for metabolic cancer therapy. J Exp Clin Cancer Res 42(1): 103, 2023. DOI: 10.1186/s13046-023-02675-4

10 Machesky LM: Deadly actin collapse by disulfidptosis. Nat Cell Biol 25(3): 375-376, 2023. DOI: 10.1038/s41556-023-01100-4

11 Yan J, Fang Z, Shi M, Tu C, Zhang S, Jiang C, Li Q, Shao Y: Clinical significance of disulfidptosis-related genes and functional analysis in gastric cancer. J Cancer 15(4): 1053-1066, 2024. DOI: 10.7150/jca.91796

12 Chen D, Li Q, Xu Y, Wei Y, Li J, Zhu X, Li H, Lu Y, Liu X, Yan D: Leveraging a disulfidptosis-related lncRNAs signature for predicting the prognosis and immunotherapy of glioma. Cancer Cell Int 23(1): 316, 2023. DOI: 10.1186/s12935-023-03147-7

13 Zhou R, Lu D, Mi J, Wang C, Lu W, Wang Z, Li X, Wei C, Zhang H, Ji J, Zhang Y, Zhang D, Wang F: Disulfidptosis-related genes serve as potential prognostic biomarkers and indicate tumor microenvironment characteristics and immunotherapy response in prostate cancer. Sci Rep 14(1): 14107, 2024. DOI: 10.1038/s41598-024-61679-y

14 Mulati Y, Lai C, Luo J, Hu J, Xu X, Kong D, Xiao Y, Liu C, Xu K: Establishment of a prognostic risk prediction model incorporating disulfidptosis-related lncRNA for patients with prostate cancer. BMC Cancer 24(1): 44, 2024. DOI: 10.1186/s12885-023-11778-2

15 Gerhauser C, Favero F, Risch T, Simon R, Feuerbach L, Assenov Y, Heckmann D, Sidiropoulos N, Waszak SM, Hübschmann D, Urbanucci A, Girma EG, Kuryshev V, Klimczak LJ, Saini N, Stütz AM, Weichenhan D, Böttcher LM, Toth R, Hendriksen JD, Koop C, Lutsik P, Matzk S, Warnatz HJ, Amstislavskiy V, Feuerstein C, Raeder B, Bogatyrova O, Schmitz EM, Hube-Magg C, Kluth M, Huland H, Graefen M, Lawerenz C, Henry GH, Yamaguchi TN, Malewska A, Meiners J, Schilling D, Reisinger E, Eils R,

Schlesner M, Strand DW, Bristow RG, Boutros PC, von Kalle C, Gordenin D, Sültmann H, Brors B, Sauter G, Plass C, Yaspo ML, Korbel JO, Schlomm T, Weischenfeldt J: Molecular Evolution of Early-Onset Prostate Cancer Identifies Molecular Risk Markers and Clinical Trajectories. Cancer Cell 34(6): 996-1011.e8, 2018. DOI: 10.1016/j.ccell.2018.10.016

16 Takashima Y, Yoshii K, Tanaka M, Tashiro K: Ubiquitin-proteasome pathway-linked gene signatures as prognostic indicators in prostate cancer. Anticancer Res 45(5): 1825-1841, 2025. DOI: 10.21873/anticanres.17562

17 Ashburner M, Ball CA, Blake JA, Botstein D, Butler H, Cherry JM, Davis AP, Dolinski K, Dwight SS, Eppig JT, Harris MA, Hill DP, Issel-Tarver L, Kasarskis A, Lewis S, Matese JC, Richardson JE, Ringwald M, Rubin GM, Sherlock G: Gene ontology: tool for the unification of biology. The Gene Ontology Consortium. Nat Genet 25(1): 25-29, 2000. DOI: 10.1038/75556

18 Dennis G Jr, Sherman BT, Hosack DA, Yang J, Gao W, Lane HC, Lempicki RA: DAVID: Database for annotation, visualization, and integrated discovery. Genome Biol 4(5): P3, 2003.

19 Takashima Y, Hamano M, Yoshii K, Hayano A, Fukai J, Iwadate Y, Kajiwara K, Hondoh H, Yamanaka R: Reciprocal expression of the immune response genes CXCR3 and IFI44L as module hubs are associated with patient survivals in primary central nervous system lymphoma. Int J Clin Oncol 28(3): 468-481, 2023. DOI: 10.1007/s10147-022-02285-8

20 Takashima Y, Sasaki Y, Hayano A, Homma J, Fukai J, Iwadate Y, Kajiwara K, Ishizawa S, Hondoh H, Tokino T, Yamanaka R: Target amplicon exome-sequencing identifies promising diagnosis and prognostic markers involved in RTK-RAS and PI3K-AKT signaling as central oncopathways in primary central nervous system lymphoma. Oncotarget 9(44): 27471-27486, 2018. DOI: 10.18632/oncotarget.25463

21 Takashima Y, Kawaguchi A, Sato R, Yoshida K, Hayano A, Homma J, Fukai J, Iwadate Y, Kajiwara K, Ishizawa S, Hondoh H, Nakano M, Ogawa S, Tashiro K, Yamanaka R: Differential expression of individual transcript variants of PD-1 and PD-L2 genes on Th-1/Th-2 status is guaranteed for prognosis prediction in PCNSL. Sci Rep 9(1): 10004, 2019. DOI: 10.1038/s41598-019-46473-5

22 Takashima Y, Kawaguchi A, Hayano A, Yamanaka R: CD276 and the gene signature composed of GATA3 and LGALS3 enable prognosis prediction of glioblastoma multiforme. PLoS One 14(5): e0216825, 2019. DOI: 10.1371/journal.pone.0216825

23 Takashima Y, Kawaguchi A, Fukai J, Iwadate Y, Kajiwara K, Hondoh H, Yamanaka R: Survival prediction based on the gene expression associated with cancer morphology and microenvironment in primary central nervous system lymphoma. PLoS One 16(6): e0251272, 2021. DOI: 10.1371/journal.pone.0251272

24 Hu G, Yao H, Wei Z, Li L, Yu Z, Li J, Luo X, Guo Z: A bioinformatics approach to identify a disulfidptosis-related gene signature for prognostic implication in colon adenocarcinoma. Sci Rep 13(1): 12403, 2023. DOI: 10.1038/s41598-023-39563-y

25 Green DR, Victor B: The pantheon of the fallen: why are there so many forms of cell death? Trends Cell Biol 22(11): 555-556, 2012. DOI: 10.1016/j.tcb.2012.08.008

26 Grubbs EG, Ng PK, Bui J, Busaidy NL, Chen K, Lee JE, Lu X, Lu H, Meric-Bernstam F, Mills GB, Palmer G, Perrier ND, Scott KL, Shaw KR, Waguespack SG, Williams MD, Yelensky R, Cote GJ: RET fusion as a novel driver of medullary thyroid carcinoma. J Clin Endocrinol Metab 100(3): 788-793, 2015. DOI: 10.1210/jc.2014-4153

27 Jiang W, Jimenez G, Wells NJ, Hope TJ, Wahl GM, Hunter T, Fukunaga R: PRC1: a human mitotic spindle-associated CDK substrate protein required for cytokinesis. Mol Cell 2(6): 877-885, 1998. DOI: 10.1016/s1097-2765(00)80302-0

28 Mollinari C, Kleman JP, Jiang W, Schoehn G, Hunter T, Margolis RL: PRC1 is a microtubule binding and bundling protein essential to maintain the mitotic spindle midzone. J Cell Biol 157(7): 1175-1186, 2002. DOI: 10.1083/jcb.200111052

29 Cantres-Velez JA, Blaize JL, Vierra DA, Boisvert RA, Garzon JL, Piraino B, Tan W, Deans AJ, Howlett NG: Cyclin-dependent kinase-mediated phosphorylation of FANCD2 promotes mitotic fidelity. Mol Cell Biol 41(8): e0023421, 2021. DOI: 10.1128/MCB.00234-21

30 Dubois EL, Guitton-Sert L, Béliveau M, Parmar K, Chagraoui J, Vignard J, Pauty J, Caron MC, Coulombe Y, Buisson R, Jacquet K, Gamblin C, Gao Y, Laprise P, Lebel M, Sauvageau G, D d'Andrea A, Masson JY: A Fanci knockout mouse model reveals common and distinct functions for FANCI and FANCD2. Nucleic Acids Res 47(14): 7532-7547, 2019. DOI: 10.1093/nar/gkz514

31 Ruan J, Zhang L, Hu D, Qu X, Yang F, Chen F, He X, Shen J, Dong K, Sweet M, Sanchez C, Li D, Shou W, Zhou J, Cai CI: Novel Myh11 dual reporter mouse model provides definitive labeling and identification of smooth muscle cells-brief report. Arterioscler Thromb Vasc Biol 41(2): 815-821, 2021. DOI: 10.1161/ATVBAHA.120.315107

32 Jo YS, Kim MS, Yoo NJ, Lee SH: Somatic mutations and intratumoral heterogeneity of MYH11 gene in gastric and colorectal cancers. Appl Immunohistochem Mol Morphol 26(8): 562-566, 2018. DOI: 10.1097/PAI.0000000000000484

33 Chen X, Ma J, Xu C, Wang L, Yao Y, Wang X, Zi T, Bian C, Wu D, Wu G: Identification of hub genes predicting the development of prostate cancer from benign prostate hyperplasia and analyzing their clinical value in prostate cancer by bioinformatic analysis. Discov Oncol 13(1): 54, 2022. DOI: 10.1007/s12672-022-00508-y

34 Frater JL, Mirkhaef M, Batanian JR: Lymphoplasmacytic lymphoma/Waldenström macroglobulinemia with inv(16)(p13q22) as a sole genetic abnormality. Cancer Genet Cytogenet 174(2): 161-165, 2007. DOI: 10.1016/j.cancergencyto.2006.11.016

35 Tochio N, Umehara T, Munemasa Y, Suzuki T, Sato S, Tsuda K, Koshiba S, Kigawa T, Nagai R, Yokoyama S: Solution structure of histone chaperone ANP32B: interaction with

core histones H3–H4 through its acidic concave domain. J Mol Biol 401(1): 97-114, 2010. DOI: 10.1016/j.jmb.2010.06.005

36 Kluth M, Galal R, Krohn A, Weischenfeldt J, Tsourlakis C, Paustian L, Ahrary R, Ahmed M, Scherzai S, Meyer A, Sirma H, Korbel J, Sauter G, Schlomm T, Simon R, Minner S: Prevalence of chromosomal rearrangements involving non-ETS genes in prostate cancer. Int J Oncol 46(4): 1637-1642, 2015. DOI: 10.3892/ijo.2015.2855

37 Srinivasan R, Mager GM, Ward RM, Mayer J, Svaren J: NAB2 represses transcription by interacting with the CHD4 subunit of the nucleosome remodeling and deacetylase (NuRD) complex. J Biol Chem 281(22): 15129-15137, 2006. DOI: 10.1074/jbc.M600775200

38 Ban F, Leblanc E, Cavga AD, Huang CF, Flory MR, Zhang F, Chang MEK, Morin H, Lallous N, Singh K, Gleave ME, Mohammed H, Rennie PS, Lack NA, Cherkasov A: Development of an androgen receptor inhibitor targeting the N-terminal domain of androgen receptor for treatment of castration resistant prostate cancer. Cancers (Basel) 13(14): 3488, 2021. DOI: 10.3390/cancers13143488

39 Liang Y, Chiu PK, Zhu Y, Wong CY, Xiong Q, Wang L, Teoh JY, Cao Q, Wei Y, Ye DW, Tsui SK, Ng CF: Whole-exome sequencing reveals a comprehensive germline mutation landscape and identifies twelve novel predisposition genes in Chinese prostate cancer patients. PLoS Genet 18(9): e1010373, 2022. DOI: 10.1371/journal.pgen.1010373

40 Bhalla S, Chaudhary K, Kumar R, Sehgal M, Kaur H, Sharma S, Raghava GP: Gene expression-based biomarkers for discriminating early and late stage of clear cell renal cancer. Sci Rep 7: 44997, 2017. DOI: 10.1038/srep44997

41 Huang SP, Bao BY, Chuang TH, Huang CY, Yu CC, Lin VC, Lu TL, Chen YT: Prognostic significance of EZH2-related gene variants in patients with prostate cancer undergoing androgen deprivation therapy. Cancer Genomics Proteomics 22(4): 611-623, 2025. DOI: 10.21873/cgp.20525

42 Nakamura N, Rogers P, Eggerson R, Post SR, Davis R: Translational research for identifying potential early-stage prostate cancer biomarkers. Cancer Genomics Proteomics 20(1): 1-8, 2023. DOI: 10.21873/cgp.20359

43 Minato A, Kudo Y, Noguchi H, Kohi S, Hasegawa Y, Sato N, Hirata K, Fujimoto N: Receptor for hyaluronic acid-mediated motility (RHAMM) is associated with prostate cancer migration and poor prognosis. Cancer Genomics Proteomics 20(2): 203-210, 2023. DOI: 10.21873/cgp.20375